
OSIRIS

Optical, Spectroscopic, and Infrared Remote Imaging System

Determination of the absolute calibration coefficients to radiometrically calibrate OSIRIS images

RO-RIS-MPAE-TN-074

Issue: 1

Revision: b

6/2/2018

Prepared by:

Cecilia Tubiana



Approval Sheet

C. Tubiana

prepared by: *Cecilia Tubiana* (signature/date)

Holger Sierks

approved by: *Holger Sierks* (signature/date)



Document Change Record

| Iss./Rev. | Date | Author | Pages affected | Description |
|-----------|-----------|------------|----------------|---|
| D / - | 5/5/2015 | C. Tubiana | all | First draft |
| 1/- | 18/6/2015 | C. Tubiana | all | First issue |
| 1/a | 22/2/2017 | C. Tubiana | Sec. 4 | Added Section 4. |
| 1/b | 6/2/2018 | C. Tubiana | Sec. 2 and 3. | Added Section 3. Clarified text and equation in Section 2. |



Table of contents

- 1 General aspects..... 1
 - 1.1 Scope 1
 - 1.2 Reference Documents 1
- 2 Absolute Calibration Coefficients 1
- 3 Camera throughput 3
 - 3.1 CCD quantum efficiency 4
 - 3.1.1 By design quantum efficiency 4
 - 3.1.2 Measured quantum efficiency of the flight CCDs..... 4
 - 3.2 Filter transmission curves 6
 - 3.3 Reflectivity of the mirrors and transmissivity of the Anti Radiation Plate (ARP) 6
 - 3.4 Data files 6
- 4 Calibration files used by OsiCalliope..... 7

List of Figures

- Figure 1 Quantum efficiency by design of the OSIRIS CCDs 4
- Figure 2 Quantum efficiency of the NAC (left) and of the WAC (right) CCD, as measured on the flight models at room temperature (295 K) and close to operational temperature (180 K). ... 5
- Figure 3 Normalized QE of the NAC at 180 K, used for the determination of the absolute calibration coefficients. 5
- Figure 4 Measured total reflectivity of the mirrors and transmissivity of the ARPs for NAC (left) and WAC (right)..... 6

List of Tables

- Table 1 Absolute calibration coefficients used for the radiometric calibration of OSIRIS images. Most of coefficients have been determined from Vega observations done in May 2014 during the post-hibernation delta calibration. The coefficients marked with asterisk have been obtained pre-hibernation. Filter is the filter combination, λ_{cent} the central wavelength of the filter, $F_{Sun,i}$ and $F_{Sun,c}$ are the solar flux integrated over the bandpass and at the central wavelength of the filter, respectively. C is the absolute calibration coefficient and error the associated uncertainty. 3
- Table 2 Quantum efficiency of the NAC and of the WAC CCD, as measured on the flight models at room temperature (295 K) and close to operational temperature (180 K)..... 5

1 General aspects

1.1 Scope

This document describes how the absolute calibration coefficients to radiometrically calibrate OSIRIS images are determined.

1.2 Reference Documents

| no. | document name | document number, Iss./Rev. |
|-----|---|----------------------------|
| RD1 | OSIRIS user manual | RO-RIS-MPAE-MA-004 D/s |
| RD2 | Pre-calibration report CCD #242 (WAC FM) | RO-RIS-MPAE-RP-073 1/- |
| RD3 | NAC CCD # 243 Acceptance Test Report | RO-RIS-MPAE-RP-355 1/- |
| RD4 | measured_13_03_01.txt (V. Da Deppo, personal communication) | |
| RD5 | Misura spettrofotometrica del trattamento ottico riflettate del 2° lotto di produzione M1-M2. | OS-GAL-TN-2001 2/0 |

2 Absolute Calibration Coefficients

Images of photometric standard stars (i.e. Vega) are used to determine the absolute calibration coefficients to radiometrically calibrate OSIRIS images. For this, the raw level 1 images are bias subtracted, flat fielded and divided by the exposure time. After the center of the star is identified, the star flux is measured with the technique of aperture photometry (using the IDL routine aper.pro). The **measured star flux** (in DN/s) is $F_{\text{star,meas}}$, and it is the *integrated flux* in the filter bandpass.

The **tabulated star flux** ($F_{\text{star,c}}$) at the central wavelength of each filter (in W/ m² nm) is extracted from the star spectra. For Vega the spectrum from the HST catalogue is used (alpha_lyr_stis_005.ascii). For 16Cyg, since it is a solar type star, the solar spectrum from the HST catalogue (sun_reference_stis_001.ascii) scaled using the 16Cyg magnitude is used.

The absolute calibration coefficients are defined as:

$$C_{\text{solar-type}} = \frac{F_{\text{star,meas}} \times k}{F_{\text{star,c}}} \left[\frac{[\text{DN/s}] \times [\text{sr}]}{[\text{W/m}^2\text{nm}]} \right]$$

where k is the pixel scale of the camera in sr ($k_{\text{WAC}} = 9.91055 \times 10^{-9}$ sr, $k_{\text{NAC}} = 3.54744 \times 10^{-10}$ sr).

If the star used for the determination of the absolute calibration coefficients is not a solar-type star, as for example Vega, the absolute calibration coefficients must be scaled to solar colors.

$$\begin{aligned} C_{\text{non-solar-type}} &= C_{\text{solar-type}} \times \frac{F_{\text{star,c}}}{F_{\text{Sun,c}}} \times \frac{\int F_{\text{Sun}}(\lambda)T(\lambda)d\lambda}{\int F_{\text{star}}(\lambda)T(\lambda)d\lambda} \\ &= \frac{F_{\text{star,meas}} \times k}{F_{\text{star,c}}} \times \frac{F_{\text{star,c}}}{F_{\text{Sun,c}}} \times \frac{\int F_{\text{Sun}}(\lambda)T(\lambda)d\lambda}{\int F_{\text{star}}(\lambda)T(\lambda)d\lambda} \end{aligned}$$



$$= k \times \frac{F_{\text{star, meas}}}{F_{\text{Sun, c}}} \times \frac{\int F_{\text{Sun}}(\lambda) T(\lambda) d\lambda}{\int F_{\text{star}}(\lambda) T(\lambda) d\lambda}$$

where:

- $F_{\text{star, c}}$ and $F_{\text{Sun, c}}$ are the flux of the star and of the Sun, respectively, at the central wavelength of the filter.
- $F_{\text{Sun}}(\lambda)$ and $F_{\text{star}}(\lambda)$ are the flux in the solar and stellar spectra, respectively. The solar and Vega spectra from the HST catalogue are used (Vega spectrum: alpha_lyr_stis_005.ascii, Solar spectrum: sun_reference_stis_001.ascii).
- $T(\lambda)$ is the throughput of the camera, including optics, filters, ARPs, and CCD. Details about the camera throughput can be found in Section 3.

To radiometric calibrate OSIRIS images acquired post-hibernation, Vega images – acquired during the delta calibration in May 2014 – have been used to determine the absolute calibration coefficients. For a few filter combinations (marked with asterisk in Table 1), no images were successfully acquitted in May 2014, thus for those filter combinations the absolute calibration coefficients determined pre-hibernation have been used.

The absolute calibration coefficients are summarized in Table 1.

| Camera | Filter | λ_{cent} (nm) | $F_{\text{Sun, i}}$ (W/m ²) | $F_{\text{Sun, c}}$ (W/m ² nm) | C ([DN/s]/[W m ⁻² sr ⁻¹ nm ⁻¹]) | Error (DN/s)/[W m ⁻² sr ⁻¹ nm ⁻¹]) |
|--------|--------|------------------------------|---|---|---|--|
| NAC | F22 | 649.20 | 71.9008 | 1.5650 | 121234824.000 | 327010.281 |
| NAC | F23 | 535.70 | 56.5356 | 1.9650 | 64300000* | 800000* |
| NAC | F24 | 480.70 | 64.3731 | 2.0300 | 61686400.000 | 955.361 |
| NAC | F26 | 360.00 | 10.7657 | 1.0205 | 12493404.000 | 162338.125 |
| NAC | F27 | 701.20 | 14.4538 | 1.4000 | 28615142.000 | 2093.743 |
| NAC | F28 | 743.70 | 37.5997 | 1.2890 | 84561712.000 | 265704.188 |
| NAC | F82 | 649.20 | 2.0161 | 1.5650 | 3278232.500 | 16708.744 |
| NAC | F83 | 535.70 | 1.6328 | 1.9950 | 1760702.250 | 851.011 |
| NAC | F84 | 480.70 | 2.0061 | 2.0600 | 1901347.375 | 7610.915 |
| NAC | F86 | 360.00 | 0.0413 | 1.0305 | 53753.266 | 606.320 |
| NAC | F87 | 701.20 | 0.6695 | 1.3950 | 1350260.500 | 1763.653 |
| NAC | F88 | 743.70 | 1.9125 | 1.2890 | 4266544.000 | 26726.639 |
| NAC | F15 | 269.30 | 0.5517 | 0.2481 | 1732428.000 | 9069.186 |
| NAC | F16 | 360.00 | 11.4451 | 1.0305 | 13394721.000 | 53132.598 |
| NAC | F81 | 600.00 | 11.7567 | 1.7790 | 14430000* | 160000* |
| NAC | F21 | 600.00 | 384.5240 | 1.7790 | 506000000* | - |
| NAC | F31 | 600.00 | 394.9301 | 1.7790 | 522000000* | - |
| NAC | F41 | 882.10 | 11.8043 | 0.9230 | 40948524.000 | 3868.637 |
| NAC | F51 | 805.30 | 11.4797 | 1.1180 | 32104672.000 | 184816.172 |
| NAC | F58 | 790.50 | 0.8919 | 1.1610 | 2300684.000 | 19645.244 |



| | | | | | | |
|-----|-----|--------|----------|--------|---------------|------------|
| NAC | F61 | 931.90 | 3.9966 | 0.8480 | 14388393.000 | 4535.661 |
| NAC | F71 | 989.30 | 1.7571 | 0.7363 | 5837449.500 | 38573.355 |
| NAC | F32 | 649.20 | 74.9988 | 1.5620 | 127300000* | 1500000* |
| NAC | F33 | 535.70 | 59.0598 | 1.9950 | 64222876.000 | 101183.891 |
| NAC | F34 | 480.70 | 67.5977 | 2.0400 | 566800000* | - |
| NAC | F35 | 269.30 | 0.1375 | 0.2481 | 486429.594 | 11019.923 |
| NAC | F36 | 360.00 | 9.3557 | 1.0305 | 10986951.000 | 597.698 |
| NAC | F37 | 701.20 | 15.0607 | 1.3900 | 30541242.000 | 1506.911 |
| NAC | F38 | 743.70 | 38.6864 | 1.2890 | 87498840.000 | 3473.541 |
| WAC | F12 | 629.80 | 162.3346 | 1.7000 | 462665440.000 | 43079.898 |
| WAC | F13 | 375.60 | 2.1484 | 1.1030 | 4794402.000 | 31081.021 |
| WAC | F14 | 388.40 | 0.9468 | 1.0195 | 2498816.000 | 17774.492 |
| WAC | F15 | 572.10 | 10.5525 | 1.8280 | 25524694.000 | 38454.344 |
| WAC | F16 | 590.70 | 3.9602 | 1.8180 | 10110339.000 | 39456.324 |
| WAC | F17 | 631.60 | 2.8359 | 1.6300 | 8595677.000 | 40090.859 |
| WAC | F18 | 612.60 | 11.3855 | 1.7090 | 31450354.000 | 40769.199 |
| WAC | F21 | 537.20 | 67.9369 | 1.8870 | 148923504.000 | 31496.266 |
| WAC | F31 | 246.20 | 0.0445 | 0.0525 | 1460941.250 | 28717.393 |
| WAC | F41 | 259.00 | 0.0317 | 0.1298 | 380327* | 6461.48* |
| WAC | F51 | 295.90 | 0.2563 | 0.5712 | 779977.438 | 24728.229 |
| WAC | F61 | 309.70 | 0.1109 | 0.5164 | 434188.312 | 32885.492 |
| WAC | F71 | 325.80 | 0.6977 | 0.9099 | 1244928.625 | 30341.326 |
| WAC | F81 | 335.90 | 0.1909 | 0.9776 | 425446.719 | 35902.289 |

Table 1 Absolute calibration coefficients used for the radiometric calibration of OSIRIS images. Most of coefficients have been determined from Vega observations done in May 2014 during the post-hibernation delta calibration. The coefficients marked with asterisk have been obtained pre-hibernation. Filter is the filter combination, λ_{cent} the central wavelength of the filter, $F_{\text{Sun},i}$ and $F_{\text{Sun},c}$ are the solar flux integrated over the bandpass and at the central wavelength of the filter, respectively. C is the absolute calibration coefficient and error the associated uncertainty.

3 Camera throughput

To calculate the throughput of the camera, the filter and ARP transmission curves, the mirror reflectivity, and the CCD quantum efficiency are used. Those files are stored in the OsiCalliope database.

The throughput of the camera is calculated using `o_filter_integrate.pro` and `o_expected_signal.pro` (Disrsoft routines). The throughput of the camera BUT filters, is calculated using `o_optics.pro`.



3.1 CCD quantum efficiency

3.1.1 By design quantum efficiency

OSIRIS NAC and WAC are equipped with (by design) identical CCDs, that are coated using “midband coating” (RD1). The quantum efficiency by design of the CCDs is shown in Figure 1.

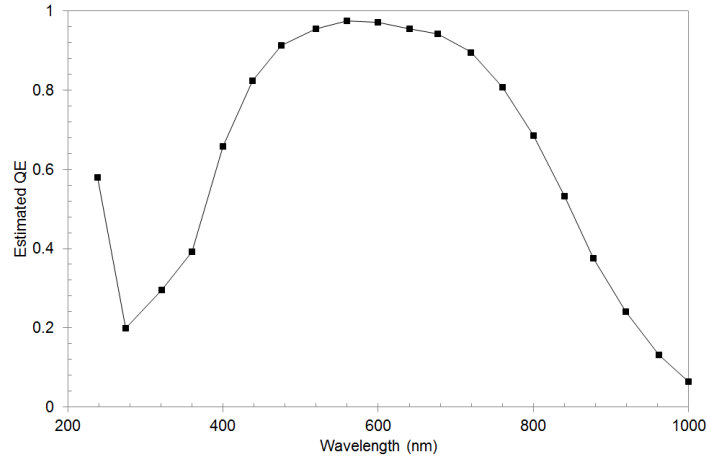


Figure 1 Quantum efficiency by design of the OSIRIS CCDs

3.1.2 Measured quantum efficiency of the flight CCDs

During the ground calibration, the quantum efficiency of the NAC (RD3) and WAC (RD2) CCDs (with $id_{NAC} = 243$ and $id_{WAC} = 242$, respectively) was measured on the flight models at room temperature (295 K) and close to operational temperature (180 K). The measured QEs are tabulated in Table 2 and shown in Figure 2.

| Wavelength (nm) | NAC CCD#243 | | WAC CCD#242 | |
|-----------------|-------------|------------|-------------|------------|
| | QE @ 295 K | QE @ 180 K | QE @ 295 K | QE @ 180 K |
| 260 | 0.342 | 0.289 | 0.343 | 0.443 |
| 280 | 0.247 | 0.205 | 0.237 | 0.291 |
| 300 | 0.311 | 0.268 | 0.289 | 0.314 |
| 320 | 0.367 | 0.308 | 0.33 | 0.333 |
| 340 | 0.415 | 0.353 | 0.363 | 0.35 |
| 360 | 0.463 | 0.388 | 0.409 | 0.358 |
| 380 | 0.585 | 0.551 | 0.5 | 0.472 |
| 399 | 0.759 | 0.742 | 0.658 | 0.629 |
| 400 | 0.754 | 0.762 | 0.668 | 0.658 |
| 449 | 0.873 | 0.891 | 0.764 | 0.743 |
| 450 | 0.868 | 0.894 | 0.779 | 0.751 |
| 500 | 0.913 | 0.969 | 0.822 | 0.815 |
| 550 | 0.928 | 0.988 | 0.829 | 0.836 |
| 600 | 0.917 | 0.974 | 0.813 | 0.821 |
| 650 | 0.89 | 0.934 | 0.785 | 0.801 |



| | | | | |
|------|-------|-------|-------|-------|
| 700 | 0.846 | 0.862 | 0.745 | 0.743 |
| 750 | 0.779 | 0.757 | 0.694 | 0.659 |
| 800 | 0.69 | 0.634 | 0.618 | 0.56 |
| 850 | 0.574 | 0.49 | 0.5 | 0.424 |
| 900 | 0.437 | 0.335 | 0.399 | 0.308 |
| 950 | 0.285 | 0.188 | 0.252 | 0.176 |
| 1000 | 0.147 | 0.075 | 0.126 | 0.067 |

Table 2 Quantum efficiency of the NAC and of the WAC CCD, as measured on the flight models at room temperature (295 K) and close to operational temperature (180 K).

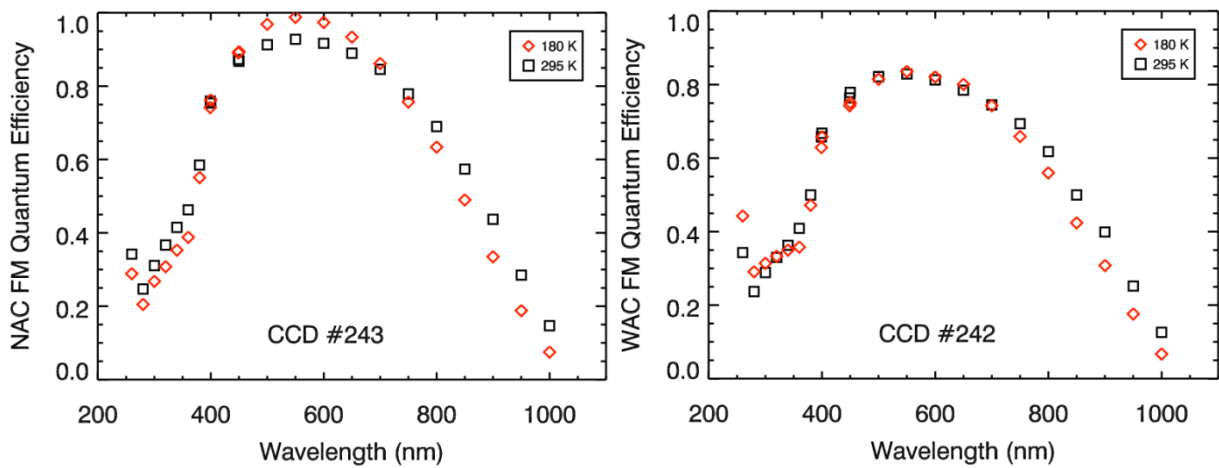


Figure 2 Quantum efficiency of the NAC (left) and of the WAC (right) CCD, as measured on the flight models at room temperature (295 K) and close to operational temperature (180 K).

For the determination of the absolute calibration coefficients, the QE of the NAC at 180 K (normalized at 650 nm) is used for both cameras (see Figure 3).

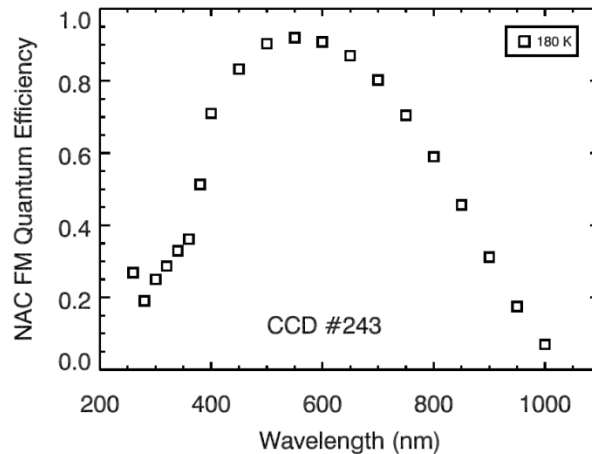


Figure 3 Normalized QE of the NAC at 180 K, used for the determination of the absolute calibration coefficients.



3.2 Filter transmission curves

Because of the characteristics of the interference filters, the filter transmission curves are CCD-position dependent. This effect is particularly significant for narrow-band filters and in case of gas line emissions. The determination of pixel-by-pixel transmission curves is undergoing.

The filter transmission curves specified by the manufacturer (and shown in Tubiana et al. 2015) are not valid for any physical pixel of the CCD.

3.3 Reflectivity of the mirrors and transmissivity of the Anti Radiation Plate (ARP)

NAC and WAC are a 3-mirrors and 2-mirrors off-axis system, respectively (RD1). The total reflectivity of the mirror system (R_{TOT}) is

$$R_{TOT} = R^N$$

where R is the reflectivity of one mirror and N the number of mirrors (i.e., $N = 2$ for WAC and $N = 3$ for NAC).

The measurement of the WAC mirror reflectivity is reported in RD5.

Both cameras are equipped with an Anti Radiation Plate (ARP), installed directly above the CCD, for radiation shielding (RD1). The measured transmissivity of the WAC APR is reported in RD4.

The total reflectivity of the mirrors and the transmissivity of the ARPs are shown in Figure 4.

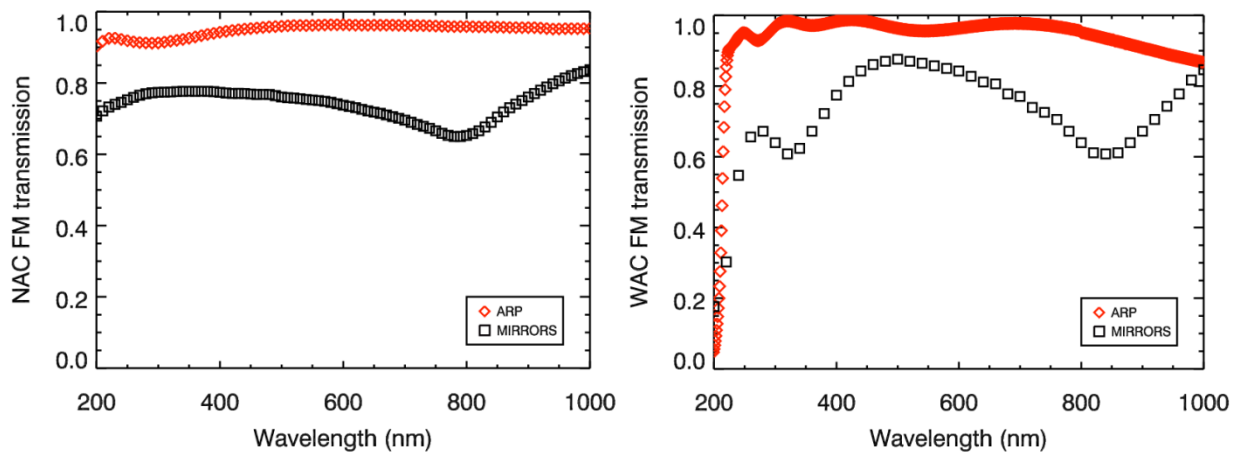


Figure 4 Measured total reflectivity of the mirrors and transmissivity of the ARPs for NAC (left) and WAC (right).

3.4 Data files

The data files used to determine the throughput of the cameras are:

- Quantum efficiency:
 - NAC_FM_QE_V01.TXT
 - WAC_FM_QE_V01.TXT
- Reflectivity of the mirrors:
 - NAC_FM_MIRROR_V01.TXT
 - WAC_FM_MIRROR_V01.TXT
- Transmissivity of the ARPs:
 - NAC_FM_ARP_V01.TXT



- WAC_FM_ARP_V01.TXT

These files are stored in the OsiCalliope database in the folder THROUGHPUT.

4 Calibration files used by OsiCalliope

The calibration files used by OsiCalliope to calibrate OSIRIS images are:

- NAC_FM_ABSCAL_V01.TXT
- WAC_FM_ABSCAL_V01.TXT

Previous versions:

- NAC_FM_ABSCAL_FACTORS.LBL (obsolete, same values as NAC_FM_ABSCAL_V01.TXT)
- WAC_FM_ABSCAL_FACTORS.LBL (obsolete, same values as WAC_FM_ABSCAL_V01.TXT)